

## Supporting Information

### Formation of an heterochiral supramolecular cage by diastereomer self-discrimination. Fluorescence enhancement and C<sub>60</sub> sensing.

Carlos Solano Arribas,<sup>a</sup> Ola F. Wendt,<sup>a</sup> Anders P. Sundin,<sup>a</sup> Carl-Johan Carling,<sup>a,b</sup> Ruiyao Wang,<sup>b</sup> Robert P. Lemieux<sup>b</sup> and Kenneth Wärnmark<sup>\*a</sup>

#### 1. Synthesis

**Generalities.** All chemicals were used as received from commercial suppliers. All moisture sensitive reactions were carried out under an atmosphere of dry nitrogen using oven-dried glassware. Flash column chromatography was performed on Matrex (25-70µm). TLC was done on aluminum sheets precoated with silica gel 60 F<sub>254</sub> (Merck). The TLC plates were visualized with Seebach stain (general), aq. KMnO<sub>4</sub> solution (for unsaturated compounds) and aq. FeCl<sub>3</sub> solution (for beta ketoesters). Melting points were determined in Electrothermal IA9000 SERIES Digital Melting Point Aparatus and were uncorrected. Optical rotations were measured on a Perkin-Elmer 341 polarimeter at 20°C. <sup>1</sup>H and <sup>13</sup>C NMR spectra were recorded on a Bruker DR400 or a Varian Unity INOVA 500 spectrometer. Chemicals shifts are given in parts per million relative to TMS using the residual solvent peaks (<sup>1</sup>H and <sup>13</sup>C NMR) and H<sub>3</sub>PO<sub>4</sub> (<sup>31</sup>P NMR).

**Improved synthesis of rac-4,10-dimethyl-2,8-bis(pyridine-4-ethynyl)-6H,12H-5,11-methanodibenzo[*b,f*][1,5]diazocene (rac-1).** To a stirred solution of rac-5 (300 mg, 0.629 mmol), CuI (4.5 mg, 0.024 mmol), Pd(PhCN)<sub>2</sub>Cl<sub>2</sub> (14 mg, 0.036 mmol) and 4-ethynylpyridine hydrochloride (336 mg, 2.40 mmol) in 1,4-dioxane (2.5 mL) was added dropwise DIPA (0.60 mL, 4.6 mmol) followed by the addition of NEt<sub>3</sub> (0.45 mL, 3.2 mmol) and 10 wt.% P(*t*Bu)<sub>3</sub> in hexanes (27 µL, 0.072 mmol). The flask was sealed under argon and the reaction mixture stirred at 60°C for 3 days. After this time, the mixture was diluted with DCM (10 mL) and washed with water (2 × 15 mL). The combined organic phases were dried over Na<sub>2</sub>SO<sub>4</sub> and the solvent evaporated under vacuum. The crude product was adsorbed on SiO<sub>2</sub> previous to column chromatography. Column chromatography on silica gel (EtOAc) afforded rac-1 (235 mg, 0.519 mmol, 86%) as a light brownish solid. All the spectroscopic data are in accordance with the previously reported.<sup>S1</sup>

**(+)-(S,S)-2,8-Diiodo-6*H*,12*H*-5,11.methanodibenzo[*b,f*][1,5]diazocine ((*S,S*)-5).** The racemic compound was synthesized according to reference S1. The two enantiomers of TB(I)<sub>2</sub> was resolved on a preparative chiral phase HPLC column, CHIRALPAK® AS®: 1.00 g of rac-5 was resolved: 40 mg in 20 ml eluent was injected at a time. The eluent mixture was 4:1 hexanes:reagent grade EtOH and the retention time, for the middle of the peaks was: Peak A = 23.2 min, Peak B = 27.6 min. Peak A, (+)-(S,S)-5, was obtained as a white solid (421mg, 0.89 mmol, 84%) ( $[\alpha]^{22}_D = +427.18^\circ$ ,  $c = 5.15$  (CHCl<sub>3</sub>)). Peak B, (-)-(R,R) 5, was obtained as a white solid (329 mg, 0.69 mmol, 66%).  $[\alpha]^{22}_D = -418.9^\circ$ ,  $c = 5.49$  (CHCl<sub>3</sub>). All the spectroscopy data are in accordance with the previously reported.<sup>S2</sup>

**rac-2,8-Bis(pyridine-4-ethynyl)-6*H*,12*H*-5,1-methanodibenzo[*b,f*][1,5]diazocine (rac-4).** This compound was synthesized in an analogous way to rac-1, with the following changes: starting from rac-2,8-bromo-6*H*,12*H*-5,11.methanodibenzo[*b,f*][1,5]diazocine (150 mg, 0.806 mmol) and tri-tert-butylphosphonium tetrafluoroborate (2.7 mg, 0.092 mmol) and 4-ethynylpyridine hydrochloride (620 mg, 4.43 mmol), yielding rac-4 (182 mg, 0.403 mmol, 50%) as an off-white solid. <sup>1</sup>H NMR (400 MHz, CD<sub>2</sub>Cl<sub>2</sub>) δ 4.25 (d,  $J = 17$  Hz, 2H), 4.36 (s, 2H), 4.74 (d,  $J = 17$  Hz, 2H), 7.09 (d,  $J = 7.40$  Hz, 2H), 7.10 (bs, 2H), 7.38 (dd,  $J = 1.6$  and 4.4 Hz, 4H), 7.40 (d,  $J = 8.4$  Hz, 2H), 8.57 (dd,  $J = 1.6$  and 4.4 Hz, 4H) ppm.

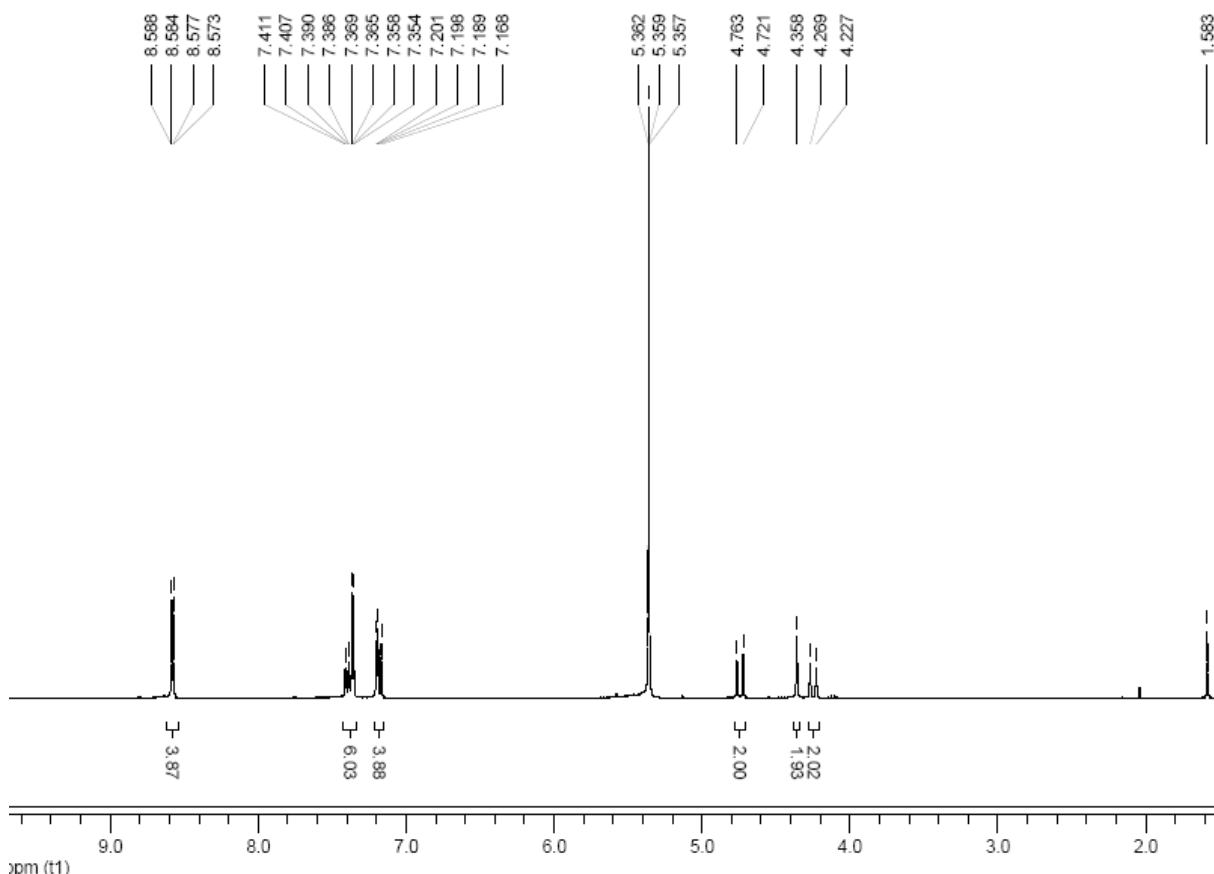


Figure S1. <sup>1</sup>H NMR (400 MHz, CD<sub>2</sub>Cl<sub>2</sub>) spectrum of rac-4.

**(+)-(S,S)-2,8-Bis(pyridine-4-ethynyl)-6H,12H-5,1-methanodibenzo[b,f][1,5]diazocene ((+)-(S,S)-4).** This compound was synthesized in an analogous way to rac-1, starting from enantiomerically pure (S,S)-5. The NMR was identical to the one for rac-4.  $[\alpha]^{20}_D = +1263^\circ$ , c 0.07 (CH<sub>2</sub>Cl<sub>2</sub>).

**(R,R,S,S)-3.** To a solution of compound rac-1 (24 mg, 0.053 mmol) in DCM (10 mL) was added (dppp)PtOTf<sub>2</sub><sup>S3</sup> (48 mg, 0.053 mmol). The solution was stirred for 28 h at rt. After this time, the solution was concentrated to half volume and the compound was precipitated by addition of diethyl ether (10 mL). The precipitate was centrifuged off to get 48 mg (66%) of product as yellow solid.  $\delta$  (202.3 MHz, CD<sub>2</sub>Cl<sub>2</sub>) -11.6 (<sup>1</sup>J<sub>P-Pt</sub> = 3058 Hz) and  $\delta$  (202.3 MHz, 1,1,2,2-tetrachloroethane-*d*<sub>2</sub>) -15.0 (<sup>1</sup>J<sub>P-Pt</sub> = 3067 Hz); <sup>1</sup>H NMR (500 MHz, 1,1,2,2-tetrachloroethane-*d*<sub>2</sub>) 2.16-2.30 (m, 4H), 2.34 (s, 12H), 3.23 (bs, 8H), 3.91 (d, *J* = 17 Hz, 4H), 4.26 (s, 4H), 4.52 (d, *J* = 17 Hz, 4H), 6.96 (s, 8H), 7.01 (bs, 4H), 7.21 (d, *J* = 5.4 Hz, 4H), 7.39 (bs, 24H), 7.60 (bs, 16H), 8.74 (d, *J* = 4.4 Hz, 8H) ppm; MS (FAB<sup>+</sup>) m/z = 2566 (M-OTf).

## 2. NMR-spectra of (*R,R,S,S*)-3.

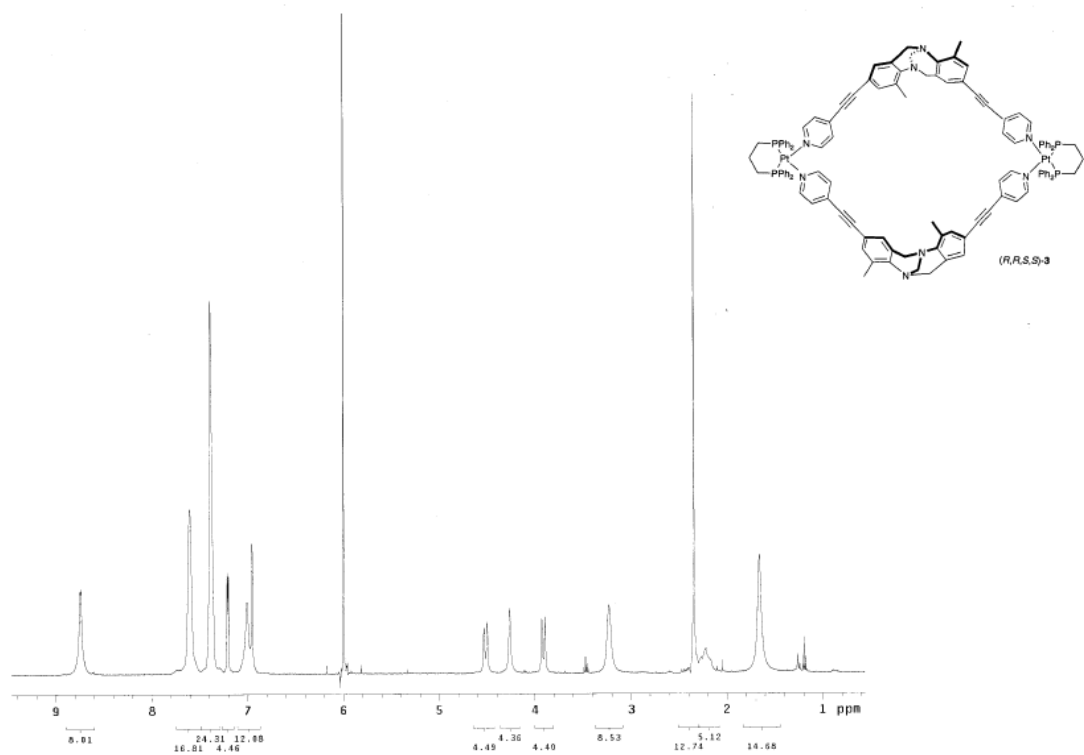


Figure S2. <sup>1</sup>H NMR (500 MHz, 1,1,2,2-tetrachloroethane-*d*<sub>2</sub>) spectrum of (*R,R,S,S*)-3 (3 mM).

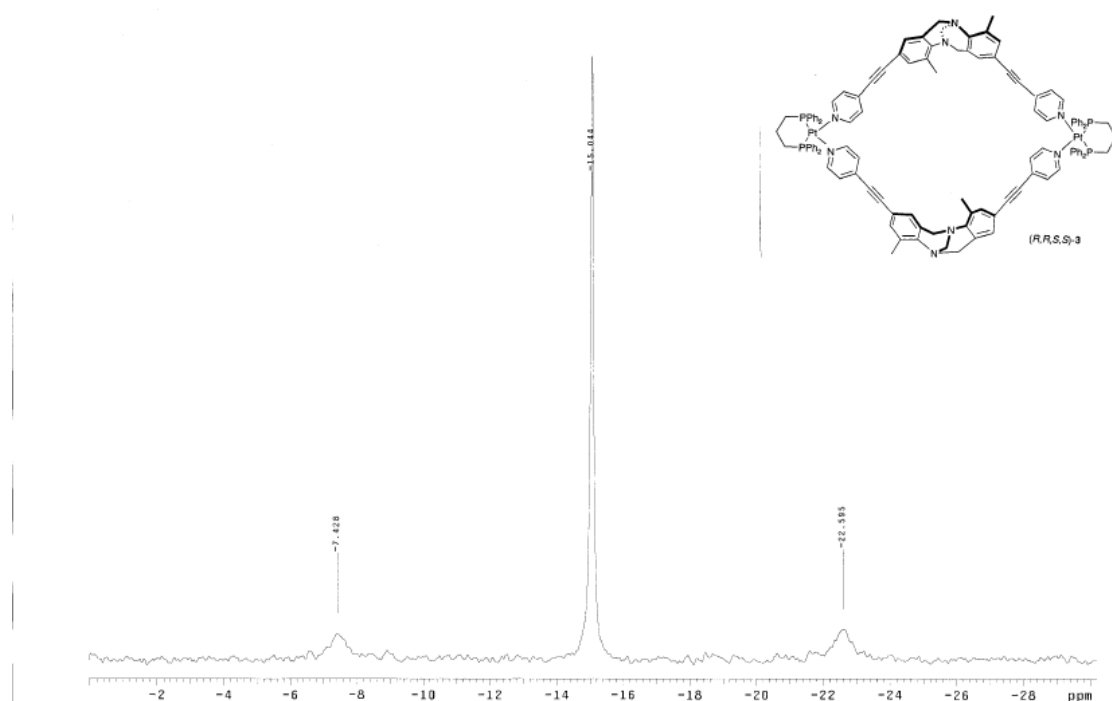


Figure S3.  $^{31}\text{P}$  (202.3 MHz,  $1,1,2,2\text{-tetrachloroethane-}d_2$ ) of  $(R,R,S,S)\text{-}3$  (3 mM).

### 3. NMR-spectra of $(R,R,S,S)\text{-}3$ and $\text{C}_{60}$ .

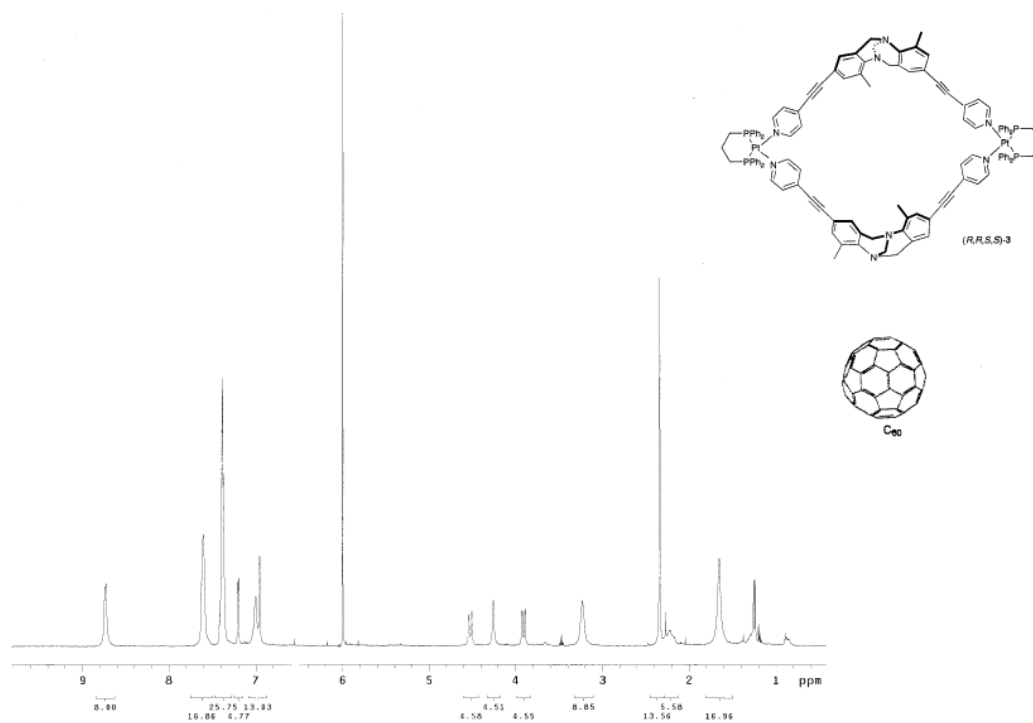


Figure S4.  $^1\text{H}$  NMR (500 MHz,  $1,1,2,2\text{-tetrachloroethane-}d_2$ ) spectrum of  $(R,R,S,S)\text{-}3$  (3 mM) and  $\text{C}_{60}$  (3 mM).

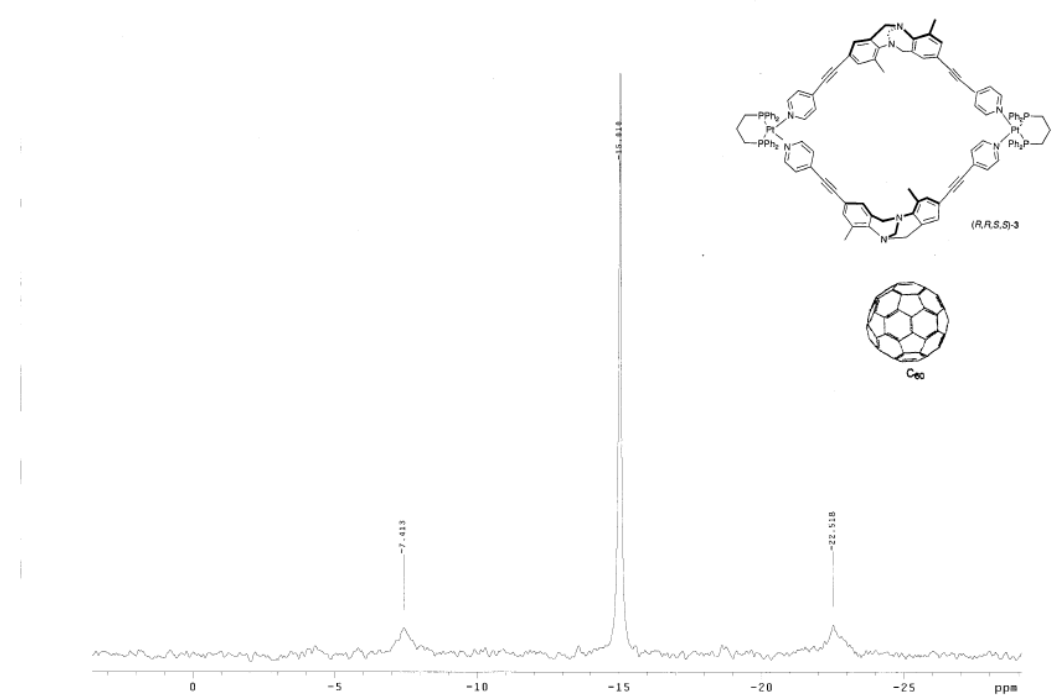


Figure S5.  $^{31}\text{P}$  (202.3 MHz, 1,1,2,2-tetrachloroethane- $d_2$ ) spectrum of  $(R,R,S,S)\text{-}3$  (3 mM) and  $\text{C}_{60}$  (3 mM).

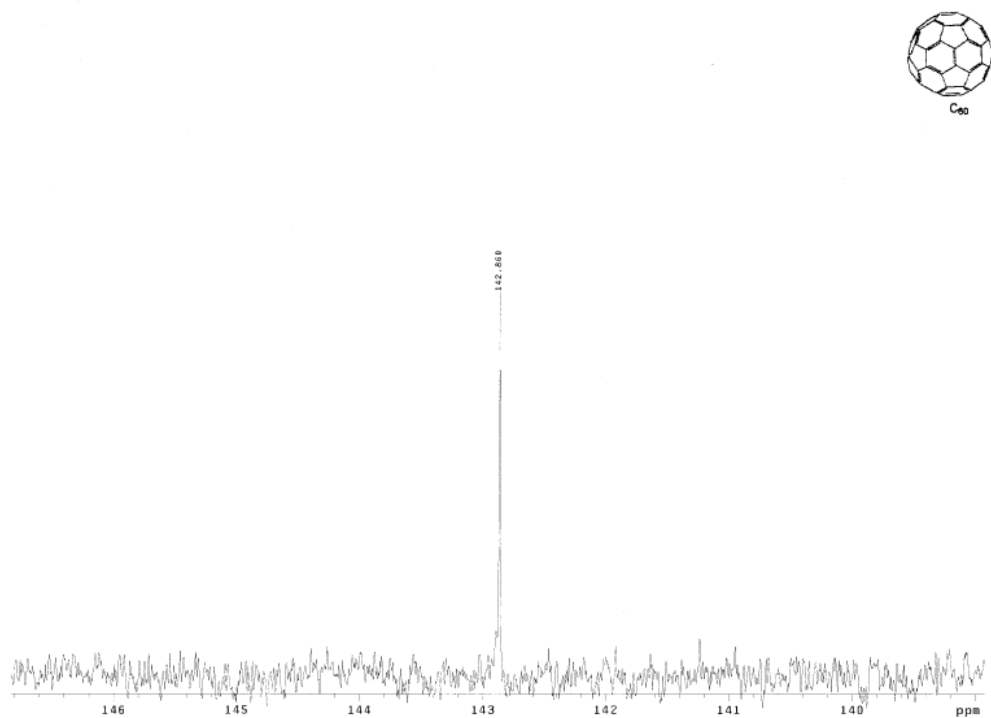


Figure S6.  $^{13}\text{C}$  (125 MHz, 1,1,2,2-tetrachloroethane- $d_2$ ) spectrum of  $\text{C}_{60}$  (3 mM).

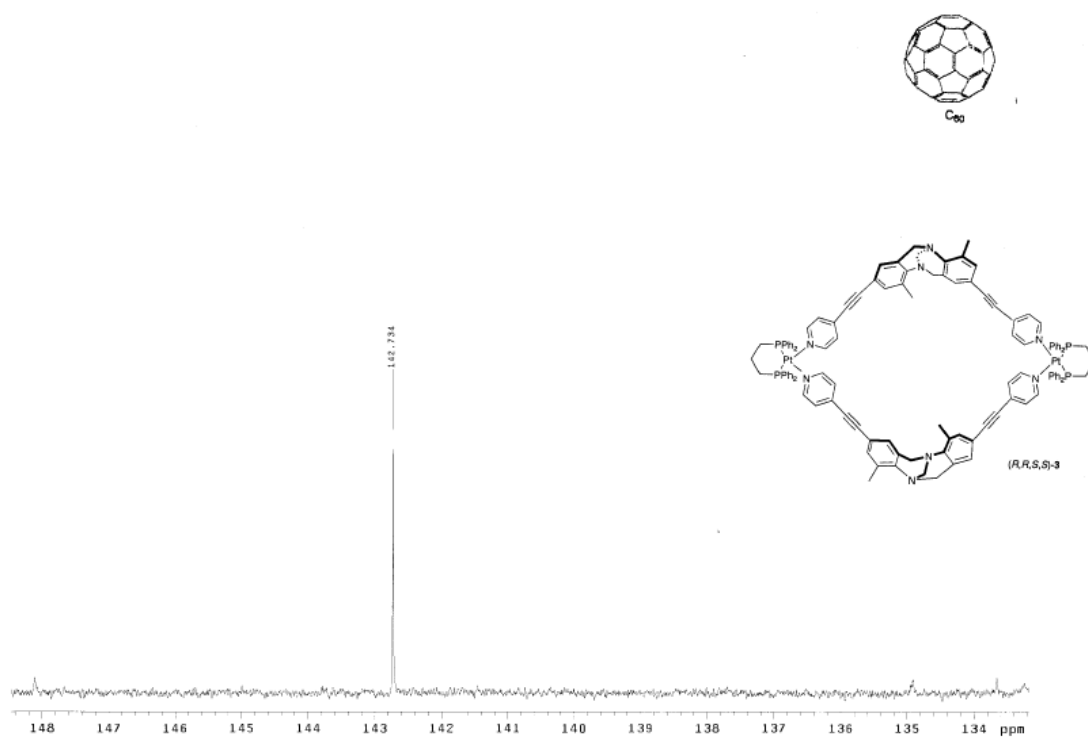


Figure S7. <sup>13</sup>C (125 MHz, 1,1,2,2-tetrachloroethane-*d*<sub>2</sub>) spectrum of C<sub>60</sub> (3 mM) and (R,R,S,S)-3 (3 mM).

#### 4. NMR of in situ formed homo- and heterochiral metallocmacrocycles

Solutions of rac-4 (3 mM) and (S,S,S,S)-4 (3 mM) in 1,1,2,2-tetrachloroethane-*d*<sub>2</sub>, respectively, were mixed with a solution 2 (3 mM) in 1,1,2,2-tetrachloroethane-*d*<sub>2</sub> to obtain a 1:1 ratio, and a few minutes later <sup>1</sup>H NMR spectra were recorded.

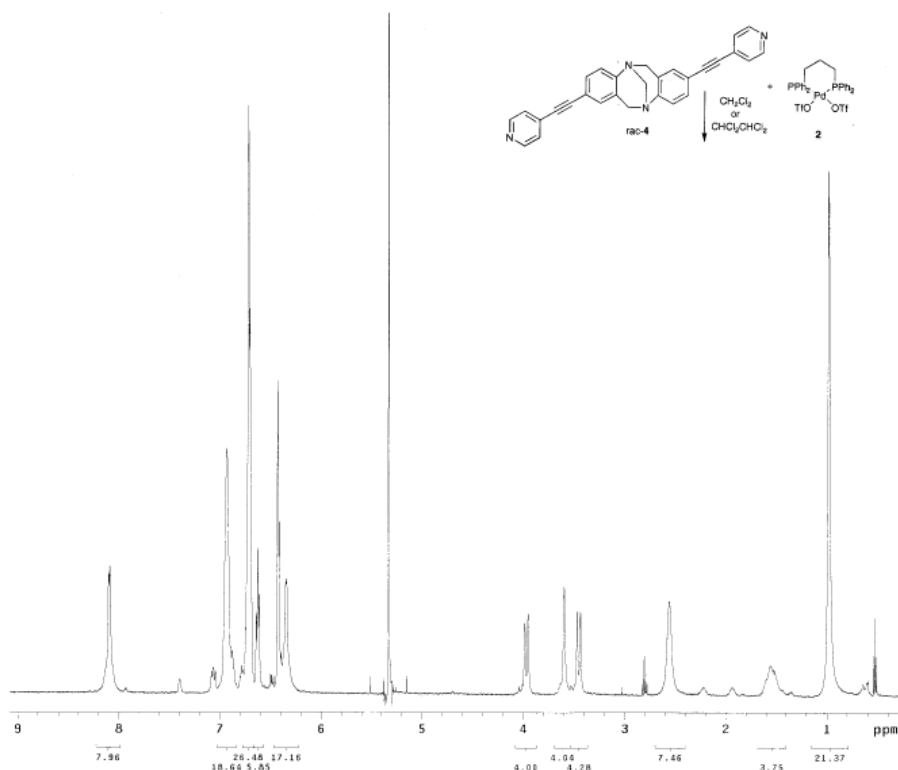


Figure S8. <sup>1</sup>H NMR (500 MHz, <sup>1,1,2,2-tetrachloroethane-d</sup><sub>2</sub>) spectrum of the metallocacyclic formed between rac-4 (3 mM) and 2 (3 mM).

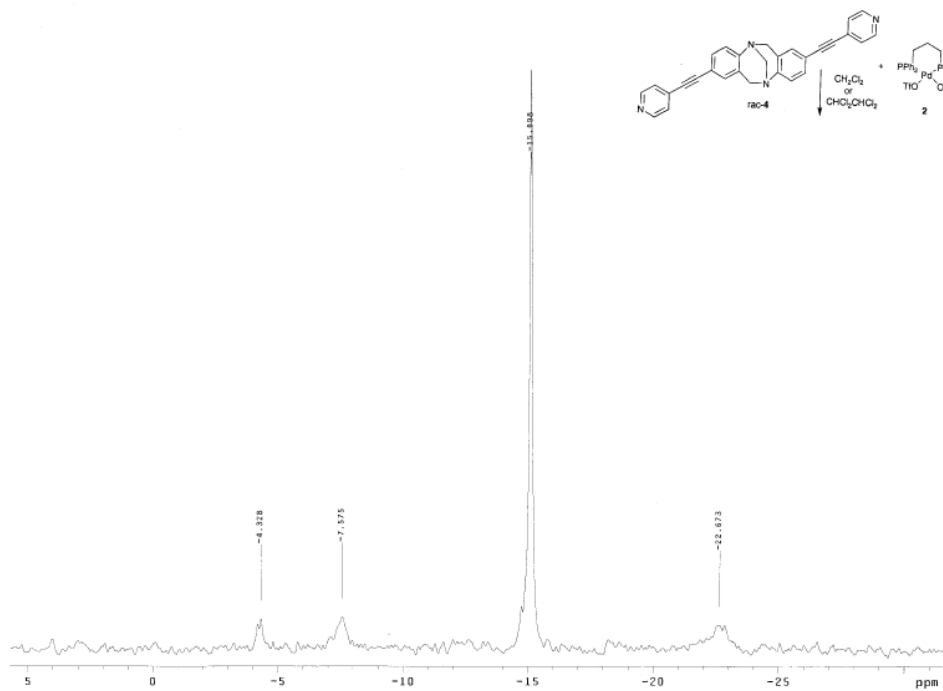


Fig. S9  $^{31}\text{P}$  (202.3 MHz, 1,1,2,2-tetrachloroethane- $d_2$ ) spectrum of the metallomacrocycle formed between rac-**4** (3 mM) and **2** (3 mM).

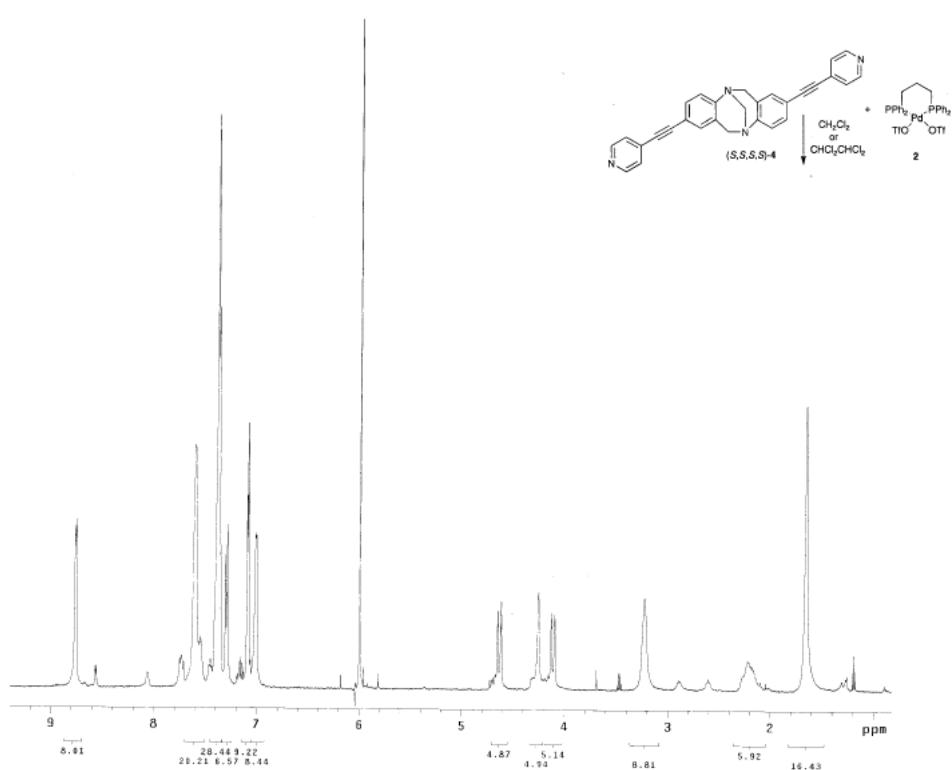


Figure S10.  $^1\text{H}$  NMR (500 MHz, 1,1,2,2-tetrachloroethane- $d_2$ ) spectrum of the metallomacrocycle formed between (*S,S,S,S*)-**4** (3 mM) and **2** (3 mM).

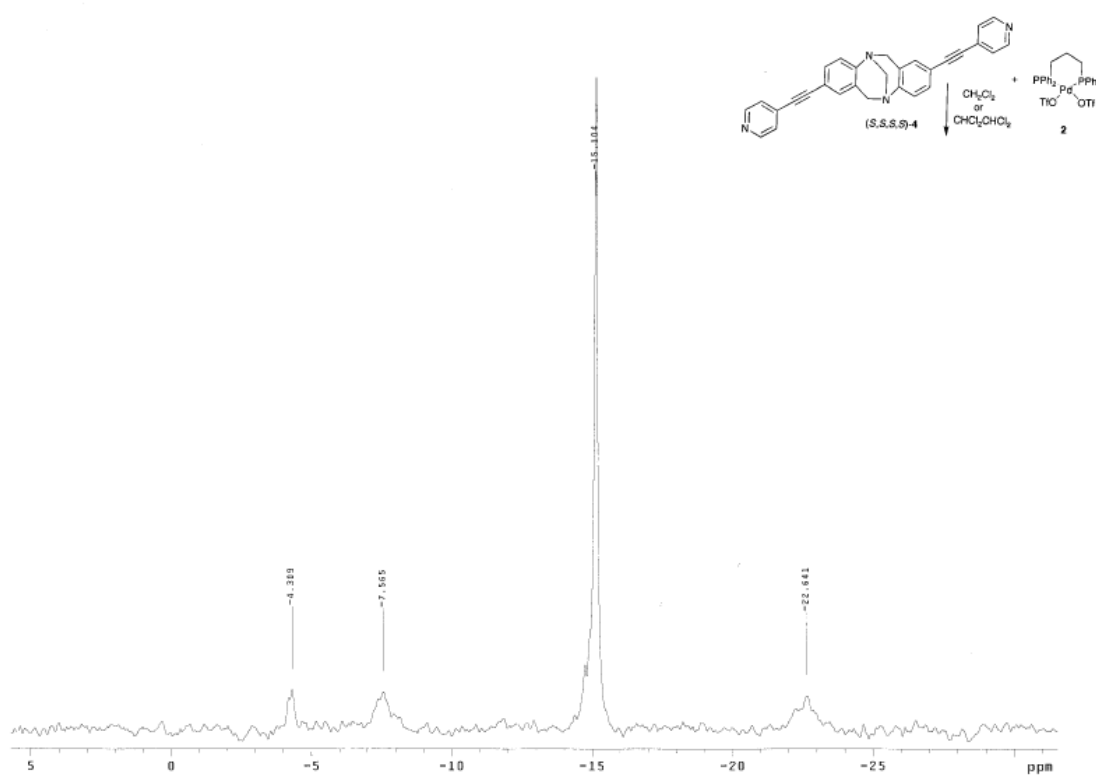


Fig. S11  $^{31}\text{P}$  (202.3 MHz, 1,1,2,2-tetrachloroethane- $d_2$ ) spectrum of the metallomacrocycle formed between  $(S,S,S,S)$ -**4** (3 mM) and **2** (3 mM).

## 5. X-ray diffraction studies

All crystallographic data is available in CIF format.

**Compound 3:** Intensity data were collected at 293K with an Oxford Diffraction Xcalibur 3 system using  $\omega$ -scans and Mo-K $\alpha$  ( $\lambda = 0.71073 \text{ \AA}$ ).<sup>S4</sup> CCD data were extracted and integrated using Crysallis RED.<sup>S5</sup> The structure was solved using direct methods and refined by full-matrix least-squares calculations on  $F^2$  using SHELXTL 5.1.<sup>S6</sup> The crystal quality was low giving weak data. Several crystals were tried but this was the best data set obtained. Thus, most non-H atoms were refined with anisotropic displacement parameters but a few were also refined isotropically. All atoms in the platinum cage could be located but the crystal also contains disordered solvent molecules. Some were modelled as isotropic dioxane molecules but the crystal also contains disordered solvent molecules. Some were modelled as isotropic dioxane moelcules and the remaining electron density was terated using a SQUEEZE procedure.<sup>S7</sup> The remaining large difference fourier peaks are located in the vicinity of the platinum atom and no further improvement was possible. Overall this gives a very poor model

with many remaining alert A's in the cif-check and the structure is only reliable insofar as connectivity is concerned. Hydrogen atoms were constrained to parent sites, using a riding model.

**Compound 5:** A crystal of the compound (+)-5 (light-brown, prism-shaped, size 0.35 x 0.15 x 0.06 mm) was mounted on a glass fiber with grease and cooled to -93 °C in a stream of nitrogen gas controlled with Cryostream Controller 700. Data collection was performed on a Bruker SMART CCD 1000 X-ray diffractometer with graphite-monochromated Mo K $\alpha$  radiation ( $\lambda = 0.71073 \text{ \AA}$ ), operating at 50 kV and 30 mA over 2 $\theta$  ranges of 6.36 ~ 50.00°. No significant decay was observed during the data collection.

Data were processed on a Pentium PC using the Bruker AXS Crystal Structure Analysis Package, Version 5.10.<sup>58</sup> The intensity data were integrated using the program SAINT-Plus. Absorption corrections were applied using program SADABS. The structure was solved by direct methods. Full-matrix least-square refinements minimizing the function  $\sum w (F_o^2 - F_c^2)^2$  were applied to the compound. All non-hydrogen atoms were refined anisotropically. The positions for all hydrogen atoms were located gradually in difference Fourier map and their contributions were included in the structure factor calculations. The solvent molecules in the lattice were disordered, and SQUEEZE was used to squeeze them out<sup>57</sup>. Two solvent accessible voids per lattice were found. Each void comprises a total volume of 218.0 Å<sup>3</sup> and contributes a total of 59.8 electrons. The void was assigned to a disordered hexane molecule, which contributes 50 electrons, and occupies about 120 Å in space. The contributions have been included in all derived crystal quantities although the precise composition of the lattice solvate is somewhat speculative.

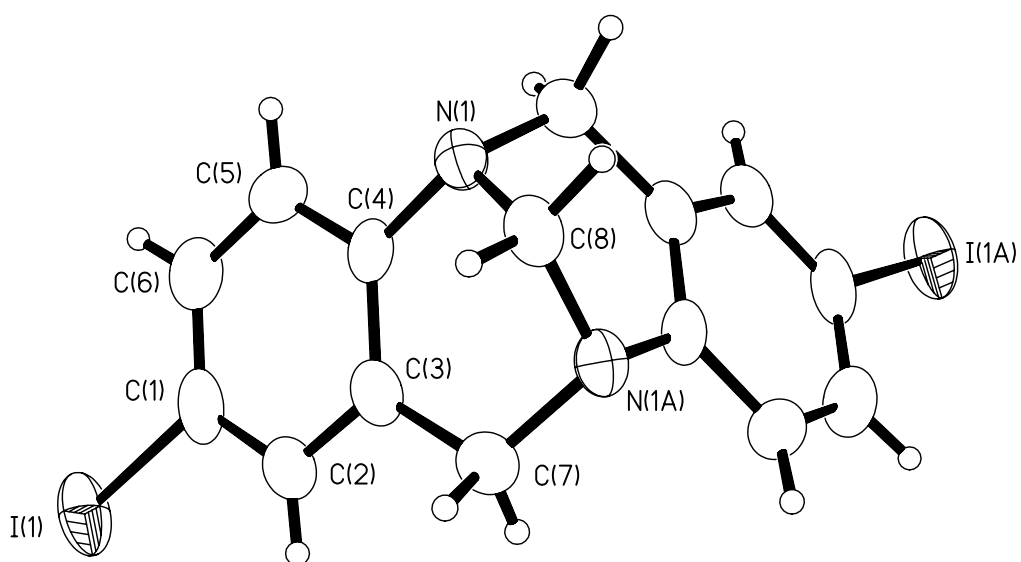


Figure S12. Molecular Structure (Displacement ellipsoids for non-H atoms are shown at the 50% probability level and H atoms are represented by circles of arbitrary size.)

## 6. Molecular modeling

To investigate the difference in stability between heterochiral (*R,R,S,S*)-**3** and homochiral (*S,S,S,S*)-**3** the two complexes were investigated by density functional theory.<sup>S9</sup> Input geometries for the DFT calculations were obtained from a conformational search using the MM3 and MMFF force fields employed in Macromodel,<sup>S10</sup> which were further refined using simple QM methods. The final DFT calculations were performed with the B3LYP functional and the LACVP\* basis set, with fully analytic SCF calculations using ultrafine grid implemented in the Jaguar program.

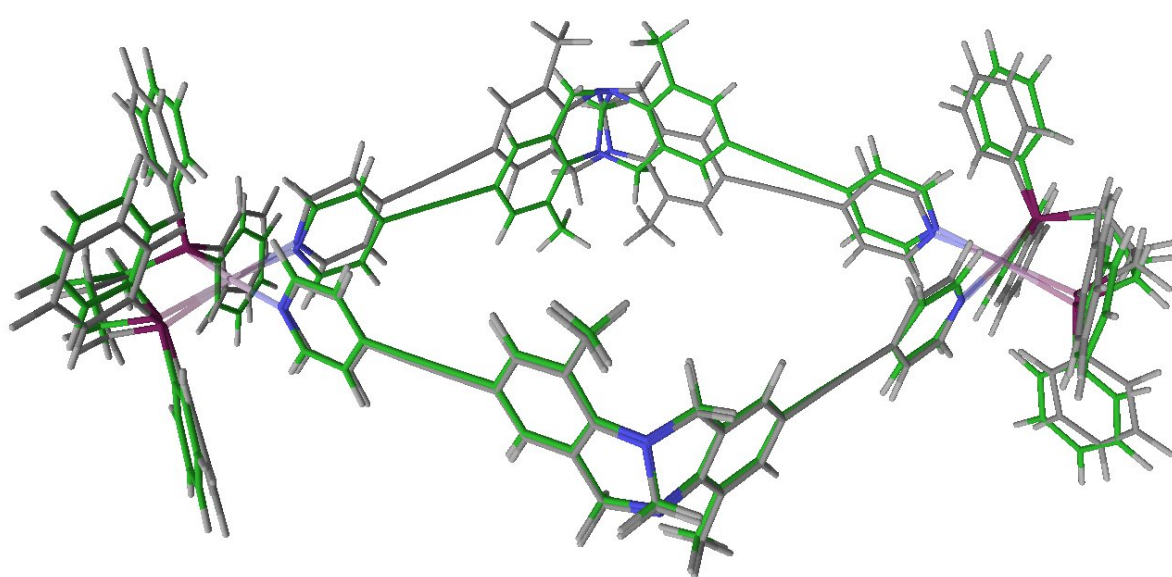


Figure S13. Results from the DFT calculations. The so obtained structures of (*S,S,S,S*)-3 (green) and (*R,R,S,S*)-3 (gray) are overlayed.

## 7. UV/VIS titration of (*R,R,S,S*)-3 with C<sub>60</sub>.

The measurements were carried out on a Carry 100 Bio UV-visible spectrophotometer.

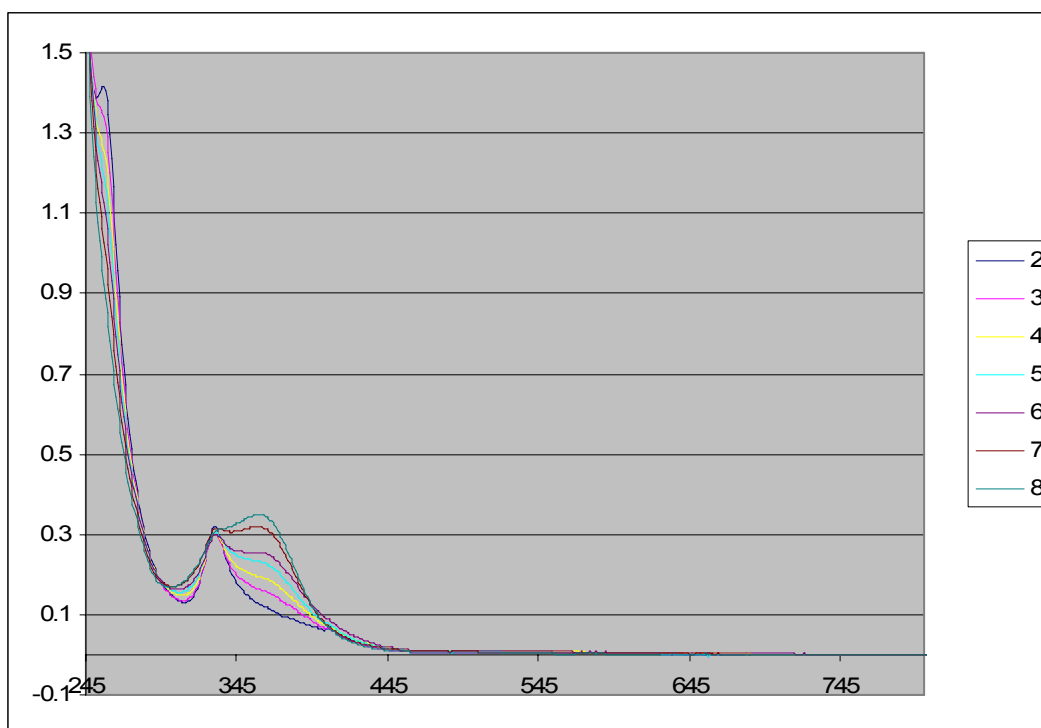


Figure S14. UV/VIS spectra (*R,R,S,S*)-**3** in 1,1,2,2-tetrachloroethane from titrations with C<sub>60</sub>. [(*R,R,S,S*)-**3** (μM)]:[C<sub>60</sub> (μM)]: line 2: 7.36:2.94; line 3: 11.0: 2.58; line 4: 14.7:2.21; line 5: 18.4:18.4; line 6: 22.1:14.7; line 7: 25.8: 11.0; line 8: 29.5:7.36.

## 8. Fluorescence titration of (*R,R,S,S*)-3 with C<sub>60</sub>.

The measurements were carried out on a Cary Eclipse fluorescence spectrometer. The competitive absorption of C<sub>60</sub> fullerene at both excitation and emission wavelengths was eliminated by calibration of the measured fluorescent intensity  $F_{exp}$  according to a literature method<sup>1</sup>. Corrections for the experimental fluorescent intensities were done according to Equation 1, where  $C_1, \varepsilon_1$  and  $C_2, \varepsilon_2$  are the concentration and molar extinction coefficients of (R,R,S,S)-3 and C<sub>60</sub> at excitation wave length ( $\lambda_{ex} = 380$  nm), respectively, while  $C_3$  and  $\varepsilon_3$  are the concentration and molar extinction coefficient of C<sub>60</sub> at emission wavelength of (R,R,S,S)-3 ( $\lambda_{em} = 380$  nm).  $l$  is the thickness of the cell.

$$F_{calc} = F_{exp} \cdot \frac{1 - e^{-\varepsilon_1 C_1 l}}{\varepsilon_1 C_1} \cdot \frac{\varepsilon_1 C_1 + \varepsilon_2 C_2}{1 - e^{-(\varepsilon_1 C_1 + \varepsilon_2 C_2) l}} \cdot \frac{\varepsilon_3 C_3 l}{1 - e^{-\varepsilon_3 C_3 l}} \quad (\text{Eq. 1})$$

A 504 μM stock solution of (R,R,S,S)-3 in 1,1,2,2 tetrachloroethane was prepared and 20 μL of this solution was diluted to 2.00 mL. The resulting solution was 5.04 μM. To this solution was added aliquots of a 504 μM stock solution of C<sub>60</sub>.

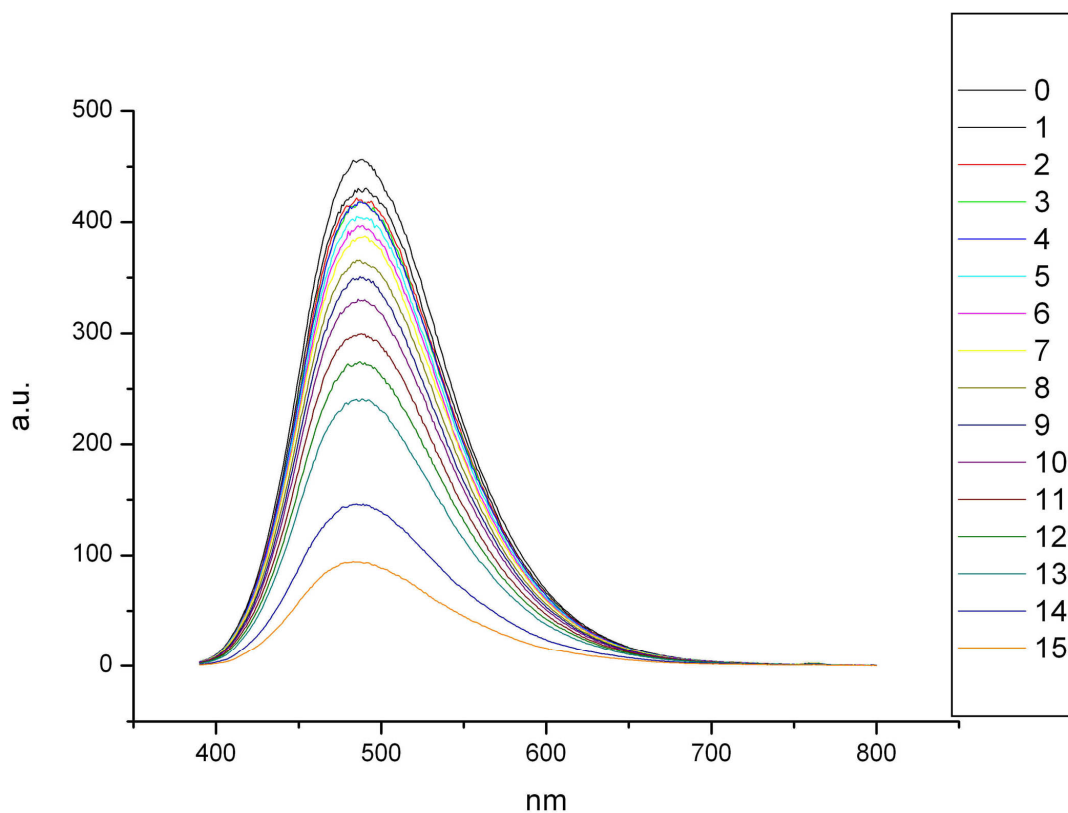


Figure S15. Fluorescence spectra of (R,R,S,S)-3 at  $\lambda_{exc} = 380$  nm in 1,1,2,2-tetrachloroethane from titrations with C<sub>60</sub>. [(R,R,S,S)-3 (μM)]:[C<sub>60</sub> (μM)]: line 0: 5.04:0;

line 1: 5.03: 1.26; line 2: 5.02:2.51; line 3: 5.01:3.75; line 4: 4.99:4.99; line 5: 4.98:6.22;  
line 6: 4.96:8.67; line 7: 4.93: 11.1; line 8: 4.90: 14.7; line 9: 4.86: 18.2; 11.0; line 10:  
4.83:21.7; line 11: 4.76: 28.5; line 12: 4.69: 35.2; line 13: 45.8:45.8; line 14: 4.20:84.0;  
line 15: 3.88: 116.

A quadratic equation (Eq. 1) was fitted to the data. where in this case  $[Q] = [C_{60}]$ .

$$F/F_0 = 1 + A[Q] + B[Q]^2 \quad (\text{Eq. 1})$$

The parameters A and B were obtained.

The quality of the fit is seen in Fig. 3. However, extracting the bimolecular association constants for static and dynamic quenching,  $K_s$  and  $K_D$ , in the Stern-Volmer equation<sup>S11</sup> (Eq. 1) failed in that the so obtaind quadratic equation gave imaginary roots.

$$F/F_0 = 1 + (K_D + K_s)[Q] + K_D K_s [Q]^2 \quad (\text{Eq. 2})$$

However, a positive deviation from the linear Stern-Volmer plot is frequently observed when the extent of quenching is large<sup>S12</sup> and the indication of an apparent static component is due to the quencher being adjacent to the fluorophore at the moment of excitation. This close fluorophore-quencher pair is immediately quenched. This view is consistent with no or only weak interaction between  $C_{60}$  and (*R,R,S,S*)-3. The slight upward deviation of the Stern-Volmer plot could also be indicative of an apparent static quenching.<sup>S11</sup> This can be interpreted in terms of a “sphere of action” in which the probability of quenching is unity. This leads to a modified Stern-Volmer equation (Eq. 3), where  $V$  is the volume of the sphere in  $\text{cm}^3$  and  $N$  is Avogados number.

$$F/F_0 = (1 + K_D)[Q] \exp([Q]VN/1000) \quad (\text{Eq. 3})$$

The quality of the fit is seen in Fig. 3. The value of  $K_D$  and  $V$  were estimated to  $(2.7 \pm 1.5) \cdot 10^3 \text{ M}^{-1}$  and  $1.2 \pm 0.2 \cdot 10^{-17} \text{ cm}^3$ , respectively, and  $R^2 = 0.998$ . From the volume, the sphere radius was calculated to  $14 \pm 2 \text{ nm}$ . Thus, the probability of quenching is 1 when  $C_{60}$  is within this distance from excited (*R,R,S,S*)-3. This distance is abnormal because that value means that the  $C_{60}$  is far from being in the vicinity of (*R,R,S,S*)-3 since the sum of the size of

the (*R,R,S,S*)-**3** and C<sub>60</sub> is around 2.5-3 nm, a value much smaller than the calculated radius of quenching.

## 9. References

- S1 J. Jensen, M. Strozyk, K. Wärnmark, *Synthesis*, 2002, 2761-2765.
- S2 (a) J. Jensen, K. Wärnmark, *Synthesis*, 2001, 1873-1877. (b) S. Sergeyev, M. Schär, P. Seiler, O. Lukoyanova, L. Echegoyen, F. Diederich, *Chem. Eur. J.*, 2005, **11**, 2284-2294.
- S3 P. J. Stang, D. H. Cao, *J. Am. Chem. Soc.*, 1994, **116**, 4981.
- S4 Crysalis CCD, Oxford Diffraction Ltd. Abingdon, Oxfordshire, UK, 2005
- S5 Crysalis RED, Oxford Diffraction Ltd. Abingdon, Oxfordshire, UK, 2005
- S6 Sheldrick, G. M. SHELXTL5.1, Program for Structure Solution and Least Squares Refinement; University of Göttingen, Göttingen, Germany, 1998.
- S7 A. L. Spek, *Acta Cryst.* **2009**, D65, 148-155
- S8 Bruker AXS Crystal Structure Analysis Package, Version 5.10 ( SMART NT (Version 5.053), SAINT-Plus (Version 6.01), SHELXTL (Version 5.1) ); Bruker AXS Inc.: Madison, WI, 1999.
- S9 Jaguar v. 6.5 release 106 from Schrodinger Inc. 2007. See <http://www.schrodinger.com>.
- S10 MacroModel v. 9.5 release 106 from Schrodinger Inc. 2007. See <http://www.schrodinger.com>; F. Mohamadi, N. G. J. Richard, W. C. Guida, R. Liskamp, M. Lipton, C. Caufield, G. Chang, T. Hendrickson, *J. Comput. Chem.*, 1990, **11**, 440.
- S11 M. Zheng, F. Bai, Y. Li, D. Zhu, *J. Appl. Polym. Sci.*, 1998, **70**, 599.
- S12 J. R. Lakowicz, *Principles of Fluorescence Spectroscopy*, 2<sup>nd</sup> Ed. Kluwer Academics, New York, 1999 p. 244.





